Optical Materials 50 (2015) 175–183

Contents lists available at ScienceDirect

Optical Materials

journal homepage: www.elsevier.com/locate/optmat

Random nanocomposites as metamaterials: Preparation and investigations at microwave region

Reza Gholipur, Ali Bahari *

Department of Solid State Physics, University of Mazandaran, Babolsar 4741695447, Iran

ARTICLE INFO

Article history:
Received 15 September 2015
Received in revised form 15 October 2015
Accepted 17 October 2015
Available online 23 October 2015

Keywords:
Random
DNMs
$Ag/Zr_{0.9}Ni_{0.1}O_y$ nanocomposite
Co-precipitation technique

ABSTRACT

$Ag/Zr_{0.9}Ni_{0.1}O_y$ nanocomposites with different atomic ratios of Ag to $Zr_{0.9}Ni_{0.1}O_y$ ($Ag/Zr_{0.9}Ni_{0.1}O_y = x$ where "x" is 0%, 5%, and 20%) were synthesized through co-precipitation technique. The structure and morphology properties of the $Zr_{0.9}Ni_{0.1}O_y$ nanocomposites were evaluated by X-ray diffraction (XRD), scanning electron microscopy (SEM), atomic force microscopy (AFM), transmission electron microscopy (TEM), and X-ray photoelectron spectroscopy (XPS) techniques. The permittivity and permeability behaviors of samples were investigated. Results showed that when 20 wt.% Ag was added (named S20), the permittivity and the permeability of the S20 became negative. These results imply the realization of double negative properties in S20 as a desired candidate for the double negative materials (DNMs).

1. Introduction

Almost all electromagnetic phenomena result from interactions between waves and materials. Creation an ordered or disordered composite artificially structured (metamaterial) is desired approach to realize a novel electromagnetic property [1,2].

The scale of inhomogeneities (the lattice constant) in an artificially structured composite is much smaller than the wavelength. Therefore, macroscopically the wave "feels" a homogeneous medium. The electromagnetic responses of this material, including the effective permittivity and permeability to external fields can be homogenized [3,4].

The metamaterial was first invented by Rodger M. Walser in 1999 [5–7]. Dielectric medium artificially structured (electric metamaterials) are usually periodic arrays of metallic wires, spheres or plates [8–10]. Other examples of metamaterials are the split-ring resonators [11,12], arrayed frequency filters [13], bianisotropic and chiral materials [14].

The structural units of metamaterials can be tailored in morphology shape and size, and their inclusions can be designed and placed in a predetermined manner to achieve prescribed functionalities. The metamaterials exhibiting tailored electromagnetic responses at optical frequencies are more fascinating [2].

Within the rapidly development of optical metamaterials, several kinds of metamaterial research have been emerging, including optical magnetism [15–17], optical DNMs [18–22], artificial chirality [23,24], nonlinear optics [25–28], super resolution [29–34], and electromagnetic cloaks [35–39].

DNMs are probably the most important section among researches of metamaterial. DNMs with simultaneously negative permittivity (ε) and permeability (μ) have attracted extensive researches in recent years because of their unique properties and potential applications of electromagnetic devices. The electromagnetic responses of a material are determined by two parameters: the ε and the μ. The ε and the μ parameters determined electromagnetic properties of the interacting electromagnetic waves [2].

Fabrication techniques for 3D ordered metal–dielectric nanostructures include direct electron-beam writing [40], focused-ion beam chemical vapor deposition [41], 3D holographic lithography [42], deep X-ray lithography [43], and multilayer nanoimprint lithography [44].

Random or disordered metal–dielectric composites confined to a thin film can be fabricated by techniques: thermal evaporation, electron-beam evaporation, and sputtering as well as electroplating [2].

Here we focus on the random metal–dielectric composites, which usually consists of the metal and dielectric components are arranged in a disordered fashion. The overall optical properties of a metal–dielectric composite can be significantly different from its constituent materials. Models for description of structures of random media are fractal structures, self-affine surfaces and percolation [45].

For random metamaterials, generalized analytical approaches are that allow us to estimate the effective electromagnetic responses of composite materials [18,46]. The response of a

* Corresponding author.
E-mail address: bahari.pa.a@gmail.com (A. Bahari).

http://dx.doi.org/10.1016/j.optmat.2015.10.018
0925-3467/

metamaterial to an electromagnetic field is dependent on the specific architecture of the meta-atoms.

Several homogenization approaches for the composites cover a wide range of methods and approximations, including a variety of field-averaging approaches, the curve-fitting approach, a dispersion-equation method, and the scattering parameter extraction method [47].

In this paper, we show that Ag metal nanowires embedded randomly in a $Zr_{0.9}Ni_{0.1}O_y$ dielectric medium can exhibit negative permittivity and negative magnetic permeability in the microwave wavelength regime. For metamaterials at microwave to infrared frequencies, silver is the metal of choice mainly because of its superior (smaller) loss factor compared. Moreover, a material with a relatively large dielectric constant is favored for the host dielectric. Therefore, in the present structure, $Zr_{0.9}Ni_{0.1}O_y$ dielectric is used.

2. Experimental

2.1. Dielectric synthesis

The $Zr_{0.9}Ni_{0.1}O_y$ nanostructural sample was prepared through co-precipitation technique using NH_4OH solution. Zirconyl chloride octahydrate [$ZrOCl_2{\cdot}8H_2O$] and nickel(II) chloride [$NiCl_2{\cdot}6H_2O$] were used as the dielectric precursors. Aqueous solutions of 1 M concentrations of zirconyl chloride octahydrate and nickel (II) chloride were prepared. NH_4OH solution was added drop wise to a beaker containing solution with 90 wt% zirconyl chloride octahydrate and 10 wt% nickel (II) chloride stirring by a magnetic stirrer.

2.2. Silver nanoparticles growth

Silver nanoparticles were synthesized by reducing $AgNO_3$ in a polyol such as ethylene glycol (EG) [$C_2H_6O_2$]. Polyvinyl pyrrolidone (PVP) was introduced as a structure directing agent. Gold nanoparticles derived by in situ pre-reducing chloroauric acid ($HAuCl_4$) in ethylene glycol were used as seeds. Firstly, $HAuCl_4$ solution was prepared from mixing of 10 mL of EG with 1 mL of 0.005 M $HAuCl_4$. A few minutes later, 170 mg of $AgNO_3$ dissolved in 10 mL of EG and 170 mg PVP dissolved in 10 mL of EG were added into $HAuCl_4$ solution with the same injection rate of 2 mL/min. This solution was stirred vigorously at 160 °C for 90 min. Silver nanowires began forming at this stage.

The solution was diluted with acetone and centrifuged at 2000 rpm for ~20 min. Ag nanoparticles were dispersed in Zr and Ni solution with different atomic ratios "*x*" (where "*x*" is 0%, 5%, and 20%) under vigorous magnetic stirring. The solution was poured into a plastic dish and sonicated for 60 min. The sample was dried at 80 °C for 24 h.

2.3. Analyses of phase and morphology

For the crystal and phase analyses, XRD measurements with Cu Kα ($\lambda = 1.5408$ Å) radiation by GBC-MMA007 (2000) were performed. Microscopy analysis and surface morphology were performed using SEM, AFM, and TEM techniques. The SEM, TEM and AFM images of the films were studied by XL30-PHILIPS, CM10-PHILIPS and LIQUID Flex AFM, respectively. The AFM images were analyzed using the DME-SPM software. Size nanostructures were also appraised by zetasizer device.

2.4. The permittivity and permeability measurements

The theories for the permittivity and permeability measurements are "parallel plate capacitor" and "inductance" methods. The parallel plate capacitor method involves sandwiching material between two electrodes to form a capacitor. The inductance method derives the permeability by measuring the inductance of the material. The concept is to wind some wire around material under test and evaluate the inductance with respect to the ends of the wire. The permittivity and permeability as functions of frequency were measured using test fixtures (Fig. 1) and GSP-730 analyzer. The test fixtures consist of material characterized by a permittivity and a permeability denoted by $\varepsilon_e = \varepsilon'_e + i\varepsilon''_e$ and $\mu_e = \mu'_e + i\mu''_e$, respectively. The real and imaginative parts of permittivity and complex permeability were determined from the following formulas [48],

$$\varepsilon'_e = \frac{Cl}{\varepsilon_0 A} \tag{1}$$

$$\varepsilon''_e = \frac{l}{RA\omega\varepsilon_0} \tag{2}$$

$$\mu_e = \frac{2\pi(L - L_0)}{\mu_0 h \ln\frac{d}{c}} + 1 \tag{3}$$

$$L = \frac{Z^*}{i\omega} \tag{4}$$

where l is the sample thickness, C the capacitance, R the resistance, A the electrode plate area, ε_0 the absolute permittivity of free space, L and L_0 are the self-inductance of toroidal test fixture with and without sample, Z^* is the complex impendence of toroidal test fixture with sample, ω is the frequency and μ_0 is the space permeability.

3. Results and discussion

3.1. XPS

The broad energy XPS spectra of the S20 sample are shown in Fig. 2. It is observed that peaks are found to be at 5.7 eV for Ag 4*d*, 59.5 eV for Ag 4*p*, 97.6 eV for Ag 4*s*, 188.2 eV for Zr 3*d*, 288.1 eV for C 1*s*, 368.5 eV for Ag 3*d*, 534.2 eV for O 1*s*, 573.2 eV for Ag $3p_{3/2}$, 603.4 eV for Ag $3p_{1/2}$ and 856.1 eV for Ni 2*p*.

3.2. XRD and size measurement

Fig. 3 presents the X-ray diffraction patterns relative to the S*x* samples with a variety doping concentration. The evolution of the crystalline structure is clearly seen when the silver molar content increases. It was also found that as the molar silver content increased, the intensity of the peaks became stronger. The S0 sample crystallises essentially in the monoclinic structure.

The five main diffraction peaks of $Zr_{0.9}Ni_{0.1}O_y$ and Ag identified with the joint committee on powder diffraction standards (JCPDS) databases (01-081-0610) and (00-001-1164), respectively, are

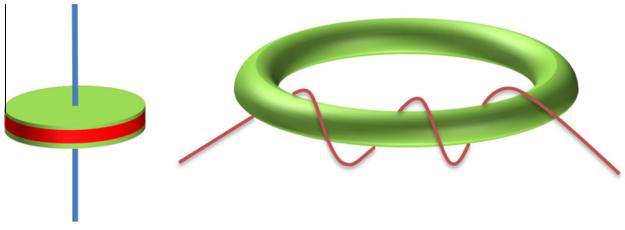

Fig. 1. The circular disc (12 mm × 2 mm; diameter *a* and thickness *l*) and toroidal test fixtures (6.5 mm × 19 mm × 2 mm; inner diameter *c*, outer diameter *d* and height *h*).